Effect of Oxygen on the Electrical Conductivity of Pt-Contacted α-Ga_2O_3/$\varepsilon(\kappa)$-Ga_2O_3 MSM Structures on Patterned Sapphire Substrates

Nikita N. Yakovlev, Vladimir I. Nikolaev, Sergey I. Stepanov, Aleksei V. Almaev, Aleksei I. Pechnikov, Evgeny V. Chernikov, and Bogdan O. Kushnarev

***Abstract*—Electrical conductivity and gas sensitivity of α-Ga_2O_3/ε (κ)-Ga_2 O_3 structures were measured for oxygen concentrations ranging from 2 % to 100 % and temperatures ranging from 25 °C to 220 °C. It was found that the oxygen sensitivity of the structures depended on the donor dopant concentration. The α-Ga_2O_3/$\varepsilon(\kappa)$-Ga_2O_3 structures doped with $\sim 1.5 \times 10^{17}$ cm^{-3} of Sn showed high sensitivity to O_2 in the temperature range from 180 °C to 220 °C and at the bias voltage below 7.5 V. This effect can be attributed to the chemisorption of oxygen molecules on the surface of structures, which reduces energy barriers between ε(k)-Ga_2O_3 grains.**

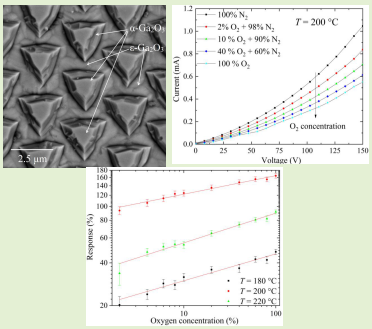

***Index Terms*—Chemisorption, ε(k)-Ga_2O_3, HVPE, *I–V* characteristic, oxygen sensor, PSS.**

I. Introduction

OXYGEN sensors are of great demand for applications in chemical and metallurgical industries [1], for monitoring and control of internal combustion engines [2], in medical devices such as in lung ventilators [3] etc. O_2 sensors based on β-Ga_2O_3 are of particular interest because they meet the requirements for miniaturization, high sensitivity, fast response, low energy consumption, and low cost [4]–[10]. The dynamic range of these sensors spans from extremely low O_2 concentrations of about 1 ppm to 100 %. In a wide temperature range from 25 °C to 900 °C, O_2 sensitivity of β-Ga_2O_3 is attributed to a reversible decrease in the electron concentration in the conduction band of a semiconductor due to chemisorption of O_2 molecules [4], [8], [9]. At higher temperatures ranging from 700 °C to 1100 °C O_2 molecules interact with oxygen vacancies in β-Ga_2O_3 [5]–[10] resulting in a reversible decrease of carrier concentration. Excellent chemical and thermal stability of β-Ga_2O_3 allows to produce gas sensors with extremely high operating temperatures of 400-1100 °C and ensures high reproducibility of their characteristics and high speed of operation. On the other hand, high operating temperature of O_2 sensors based on β-Ga_2O_3 can be seen as a major drawback because it increases the energy consumption. The operating temperature of O_2 sensors based on β-Ga_2O_3 can be reduced by doping [4], [11] or by using nanostructures [4], [12]. Often, a relatively small reduction in operating temperature leads to a noticeable decrease in the speed of response and long-term drift of their characteristics.

Previously, we studied the effect of H_2 on the electrical conductivity and gas-sensing properties of α-Ga_2O_3/$\varepsilon(\kappa)$-Ga_2O_3 structures with Pt contacts grown by the halide vapor phase epitaxy (HVPE) on the patterned sapphire substrates (PSS) [13]. These structures showed a response to H_2 starting from room temperature. The minimum detectable concentration of H_2 at a temperature of 125 °C was 54 ppm. At high bias voltages, α-Ga_2O_3/$\varepsilon(\kappa)$-Ga_2O_3 structures with Pt contacts showed a significant response to O_2 and NH_3. However, at bias voltages lower than 7.5 V the sensors showed no response to CH_4, O_2, CO, and NH_3. The sensitivity of structures to H_2 was attributed to the variation of the potential barrier height at the Pt/$\varepsilon(\kappa)$-Ga_2O_3 interface.

Manuscript received March 31, 2021; accepted April 8, 2021. Date of publication April 12, 2021; date of current version June 30, 2021. This work was supported by the Russian Science Foundation under Project 20-79-10043. The associate editor coordinating the review of this article and approving it for publication was Prof. Yu-Cheng Lin. *(Corresponding author: Aleksei V. Almaev.)*

Nikita N. Yakovlev, Aleksei V. Almaev, Evgeny V. Chernikov, and Bogdan O. Kushnarev are with the Research and Development Centre for Advanced Technologies in Microelectronics, National Research Tomsk State University, 634050 Tomsk, Russia (e-mail: nik_mr_x@mail.ru; almaev_alex@mail.ru; evvch192184@gmail.com; kuschnaryow@mail.ru).

Vladimir I. Nikolaev, Sergey I. Stepanov, and Aleksei I. Pechnikov are with the Perfect Crystals LLC, 194064 Saint Petersburg, Russia, and also with the Ioffe Institute of the Russian Academy of Sciences, 194021 Saint Petersburg, Russia (e-mail: nkvlad@inbox.ru; s.i.stepanov@googlemail.com; alpechn@yandex.ru).

Digital Object Identifier 10.1109/JSEN.2021.3072664

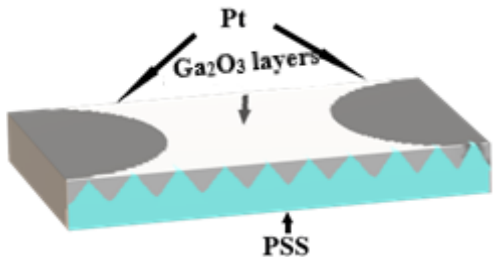

Fig. 1. Schematic illustration of a sensor based on the Pt contacted Ga_2O_3 film grown on PSS.

It may be reasonably assumed that the sensitivity of α-Ga_2O_3/$\varepsilon(\kappa)$-Ga_2O_3 to certain gases, in particular oxygen, depends on the doping level. In this work we investigate the effect of O_2 on the conductivity of α-Ga_2O_3/$\varepsilon(\kappa)$-Ga_2O_3 structures doped with reduced concentration of Sn dopant.

II. Experimental Methods

The Ga_2O_3 films investigated in this paper were produced by Perfect Crystals LLC using the HVPE method. The films were deposited on 430 micron thick PSS of (0001) orientation. The surface of the PSS was formed by a regular array of protruding cones arranged in a hexagonal lattice. An in-depth report on the structural properties and chemical composition of the epitaxial films can be found elsewhere [14].

The surface morphology of the films was studied using a Tescan MIRA 3 LMU scanning electron microscope (SEM). Pt contacts of 340-360 nm thickness were formed on the surface of Ga_2O_3 layers by vacuum deposition through a mask. Then, the wafers were diced into 1 mm × 1.85 mm size chips. A schematic layout of the test chip is shown in Fig. 1.

Fig. 2 shows a photograph of a setup used to measure the effect of O_2 on the electrical properties of Ga_2O_3 layers. The setup consisted of a hot stage with electrical probes placed inside a sealed metal chamber of 950 cm^3 in volume. The temperature of the hot stage was controlled by a programmable Rigol DP-832 DC power source. A mixture of N_2 and O_2 gases was pumped through the chamber. The concentration of O_2 in the chamber was controlled using a "Microgas F-06" gas mixing and delivery system equipped with Bronkhorst El-Flow F 201CV mass flow controllers. The total flow of the gas mixture was maintained at a constant rate of 1000 sccm. A Keithley 2636A source-meter was used to measure current-voltage (I–V) characteristics and time dependencies of current at various experimental conditions. An Agilent E4980A RLC meter was used to measure the capacitance-voltage (C-V) and capacitance-frequency (C-f) characteristics.

III. Results and Discussion

A. Structural analysis

X-ray diffraction (XRD) analysis was used to determine the phase composition of the Ga_2O_3 epitaxial layers. The XRD spectra of the Ga_2O_3 films showed peaks at $2\theta = 40.25°$ and $2\theta = 87.05°$ corresponding to (0006) and (0.0.0.12) of α-Ga_2O_3 reflections. In addition to the diffraction peaks of α-Ga_2O_3, characteristic peaks of $\varepsilon(\kappa)$-Ga_2O_3 were observed

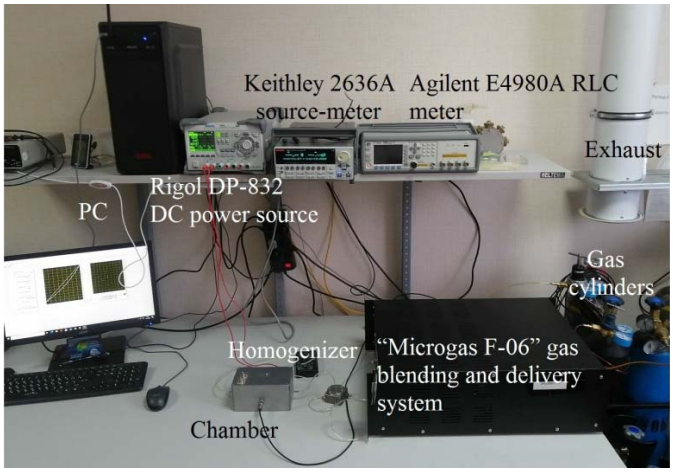

Fig. 2. Photograph of the setup for measuring the effect of O_2 on electrical properties of Ga_2O_3 films.

at 19.18°, 38.89°, 59.90°, 83.48° and 112.63° corresponding to (0002), (0004), (0006), (0008) and (0.0.0.10) reflections, respectively. Thus, the samples consisted of a mixture of α and $\varepsilon(\kappa)$ phases with the (0001) orientation. A more in-depth analysis of the structural properties of the Ga_2O_3 films can be found in Ref. [14]. Optical transmission measurements also confirmed the presence of $\varepsilon(\kappa)$-Ga_2O_3 phase with a narrower bandgap ($E_g = 4.82$ eV) and α-Ga_2O_3 with a wider bandgap ($E_g = 5.06$ eV). Fig. 3 shows a representative plan-view and cross-sectional SEM images of a α-Ga_2O_3/$\varepsilon(\kappa)$-Ga_2O_3 structure. One can see that the α-phase forms columnar structures at the top of the sapphire cones, and the $\varepsilon(\kappa)$-phase fills the gaps between the columns. The characteristic triangular shape of columnar structures also indicates that they consist of α-Ga_2O_3 with trigonal symmetry. The length of the base edges of α-Ga_2O_3 pyramidal structures is 2.6-2.8 μm. Also, SEM images show the presence of interfaces between neighboring $\varepsilon(\kappa)$-Ga_2O_3 crystal blocks of around the α-Ga_2O_3 columnar structures. The mean size of $\varepsilon(\kappa)$-Ga_2O_3 crystal blocks varies between 3.2 and 4.0 μm. Thus it can be concluded that the $\varepsilon(\kappa)$-Ga_2O_3 phase has a granular structure.

B. Electrical conductance of α-Ga_2O_3/$\varepsilon(\kappa)$-Ga_2O_3 structures under pure dry air and dry N_2

Pt is known to form a Schottky barrier contact with α-Ga_2O_3 and $\varepsilon(\kappa)$-Ga_2O_3 [15], [16]. Thus, the test structures can be viewed as two Schottky diodes connected reversely in series. The semiconductor layer between the Pt contacts can be represented as a series resistance. The equivalent circuit of α-Ga_2O_3/$\varepsilon(\kappa)$-Ga_2O_3 structure with Pt contacts is shown in Fig. 4. According to the model of two Schottky diodes [17], the current through the α-Ga_2O_3/$\varepsilon(\kappa)$-Ga_2O_3 structure with Pt contacts is determined by the reverse-biased barrier and saturates with increasing applied voltage. Analytical equations describing I–V characteristics of α-Ga_2O_3/$\varepsilon(\kappa)$-Ga_2O_3 MSM structures can be found in our previous work [13]. The I–V characteristics of MSM structures may depart from a typical I–V curve of a reverse-biased Schottky barrier when the resistance of the semiconductor layer substantially exceeds the resistance of the space charge region (SCR). As it was

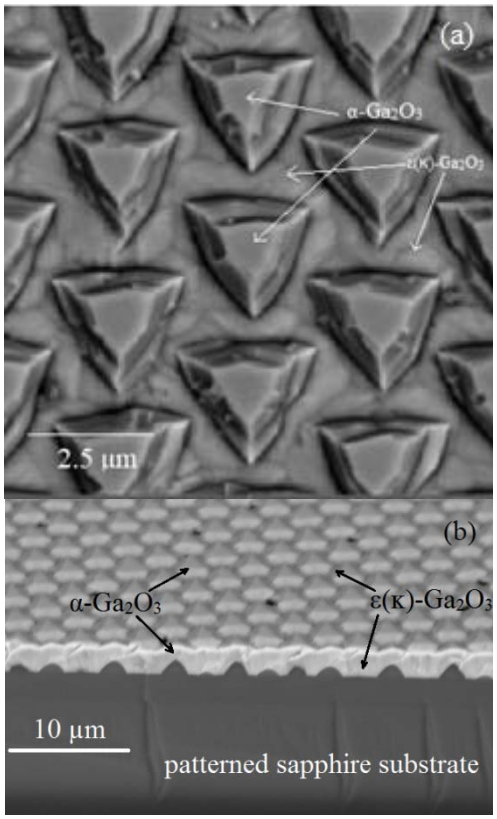

Fig. 3. SEM plan-view (a) and SEM cross-sectional view (b) images of α-Ga_2O_3/$\varepsilon(\kappa)$-Ga_2O_3 structures on PSS.

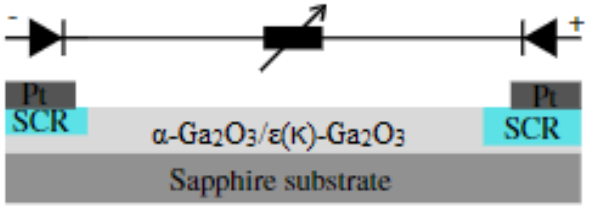

Fig. 4. Model of the α-Ga_2O_3/$\varepsilon(\kappa)$-Ga_2O_3 structure with Pt contacts.

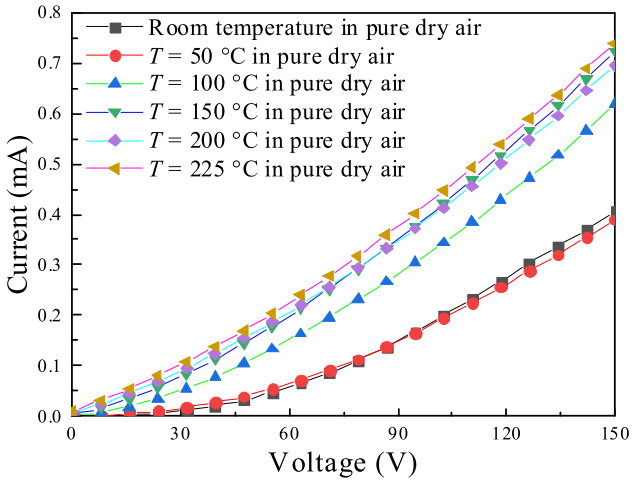

Fig. 5. *I–V* characteristics of α-Ga_2O_3/$\varepsilon(\kappa)$-Ga_2O_3 with Pt contacts in an atmosphere of pure dry air.

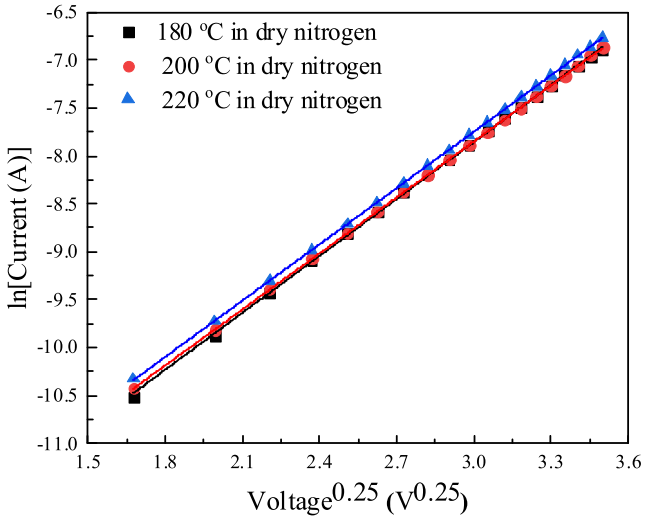

Fig. 6. *I–V* characteristics of α-Ga_2O_3/$\varepsilon(\kappa)$-Ga_2O_3 with Pt contacts in dry N_2 atmosphere.

pointed out by Elhadidy *et al.* [18], the shape of *I–V* curve is determined by the ratio between the resistances of the semiconductor bulk and space charged region of the reverse-biased barrier.

The *I–V* characteristics of the structures are determined by the reverse-biased barrier at the metal/semiconductor interface and the resistance of the semiconductor bulk. Fig. 5 shows the *I–V* characteristics of samples under a dry air atmosphere at various temperatures. One can see that the current does not saturate with increasing bias due to the high resistance of the semiconductor layer. Also, at any fixed bias, the current slightly increases with temperature increasing from 25 °C to 225 °C. This effect can be explained by the temperature dependence of the current through the reverse-biased Schottky barrier and the generation of charge carriers in the semiconductor layer. A plot of $ln(I)$ vs $U^{1/4}$ (Fig. 6) gives a linear relationship in the bias ranging from 0 V to 150 V. This is consistent with the model of current conduction in MSM structures based on the thermionic emission theory in the diode approximation [18]. The slope of the plot corresponds to the donor concentration N_d of about 1.5-2.1 $\times$ 10^{17} cm^{-3}, which is in good agreement with N_d value obtained from *C-V* measurements. It is worth noting that the N_d for the samples with high sensitivity to H_2 and current saturation at high bias is about 20 times higher [13].

The *C-f* characteristics were measured in the frequency range from 20 Hz to 1 MHz in dry N_2 atmosphere. The capacitance of the α-Ga_2O_3/$\varepsilon(\kappa)$-Ga_2O_3 structures decreases monotonically with an increase in frequency f from 1 kHz to 1 MHz, which indicates a small contribution of deep electronic levels. The *C-f* characteristics showed a plateau for frequencies up to 1 kHz. The results of *C-f* measurements are consistent with published reports [19], [20].

Previously [21], we investigated the gas sensing properties of α-Ga_2O_3/$\varepsilon(\kappa)$-Ga_2O_3 structures with N_d $<10^{15}$ cm^{-3}. These samples were insensitive to most of the gases except water vapor for which they exhibited significant sensitivity in the temperature range from 25 °C to 100 °C.

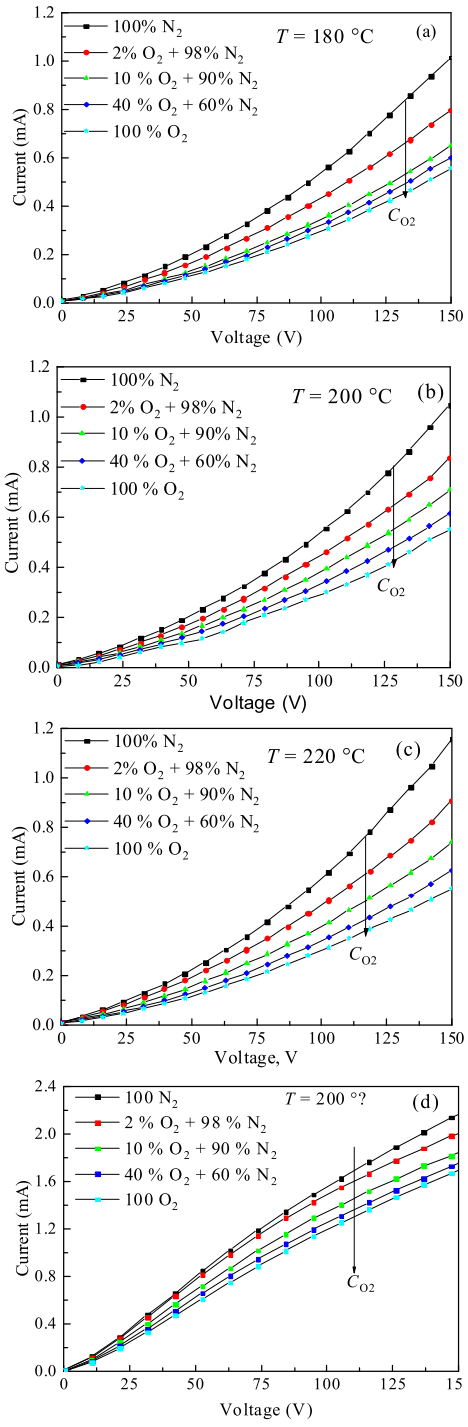

Fig. 7. *I–V* characteristics of α-$Ga_2O_3/\varepsilon(\kappa)$-$Ga_2O_3$ MSM structures with Pt contacts upon the exposure to different concentrations of O_2 at $N_d = 1.5\text{-}2.1 \times 10^{17}$ cm^{-3} and $T = 180$°C (a), $T = 200$°C (b), $T = 220$°C (c), (d) at $N_d = 4 \times 10^{18}$ cm^{-3} and $T = 200$ °C.

C. Electrical conductance of α-$Ga_2O_3/\varepsilon(\kappa)$-$Ga_2O_3$ structures at O_2 exposure

Fig. 7 a-c show the *I–V* characteristics of α-$Ga_2O_3/\varepsilon(\kappa)$-$Ga_2O_3$ structures with N_d =1.5-2.1 × 10^{17} cm^{-3} at different temperatures upon the exposure to O_2 at concentrations ranging from 0 to 100 %. The *I–V* characteristics of α-$Ga_2O_3/\varepsilon(\kappa)$-$Ga_2O_3$ structures with $N_d = 4 \times 10^{18}$ cm^{-3} at $T = 200$ °C are shown in Fig. 7 d. The zero O_2 concentration corresponds to pure N_2 atmosphere. The *I–V* characteristics of the samples were measured after a 10 minute exposure to each O_2 concentration C_{O2}. It can be seen that current decreases with increasing O_2 concentration. The effect of O_2 on the *I–V* characteristics of structures with an increased Sn concentration is much weaker and this trend is observed at all selected temperatures. Therefore, below we will consider the structures with $N_d = 1.5 - 2.1 \times 10^{17}$ cm^{-3}.

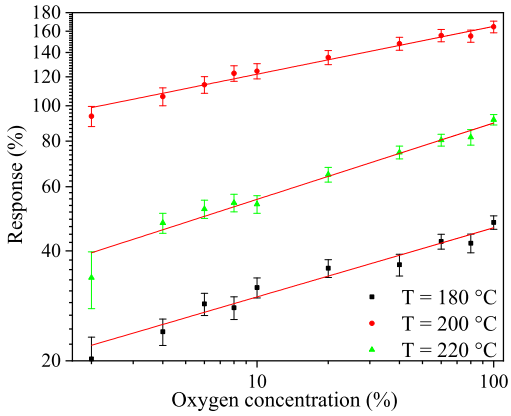

Fig. 8. Response versus O_2 concentration at the temperatures of 180, 200 and 220 °C.

TABLE I
EXPONENT B AT VARIOUS TEMPERATURES

T, °C	*b*
180	0.19±0.01
200	0.130±0.006
220	0.21±0.01

The relative sensor response was calculated using the following formula:

$$S = \frac{I_{N2} - I_{O2}}{I_{N2}} \times 100\% = \frac{\Delta I}{I_{N2}} \times 100\%, \qquad (1)$$

where I_{N2} is the quasi-stable value of the current in pure N_2 atmosphere; I_{O2} is the quasi-stable current when exposed to N_2+ O_2 gas mixture. Concentration dependences of the O_2 response at 7.5 V bias are shown in Fig. 8.

The highest response to O_2 was observed at 200 °C over the whole span of O_2 concentrations. It is worth noting that this temperature is significantly lower than the operating temperature of oxygen sensors based on the β-Ga_2O_3. High sensitivity to oxygen at relatively low temperatures α-$Ga_2O_3/\varepsilon(\kappa)$-$Ga_2O_3$ is a considerable advantage since it allows to produce gas sensors with low energy consumption. The response of structures with $N_d = 4 \times 10^{18}$ cm^{-3} was much lower and, for example, at $C_{O2} = 40$ % does not exceed 49.3 % in the temperature range of 180-220 °C.

The dependence of the response versus O_2 concentration in the range of C_{O2} from 2 % to 100 % can be fairly accurately approximated by a power function $S \sim C_{O2}^{b}$, where b is the exponent that depends on the temperature (Table I).

Fig. 9 shows the response versus the applied bias voltage. In the range of tested temperatures, the response shows a weak dependence on applied bias. Thus, for the investigated

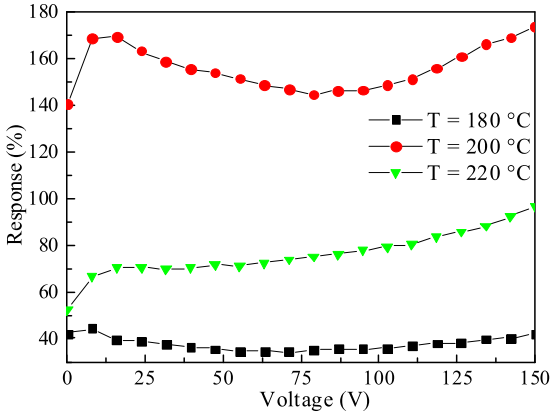

Fig. 9. Response versus bias voltage at C_{O2} = 10 % and T = 180 °C, 200 °C and 220 °C.

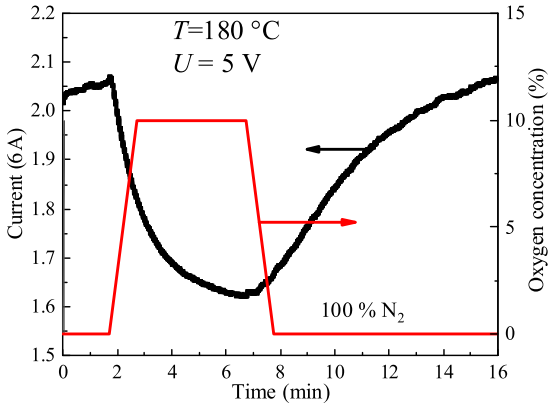

Fig. 10. Time dependences of the current at C_{O2} = 10% and the O_2 concentration in the chamber.

α-Ga_2O_3/$\varepsilon(\kappa)$-Ga_2O_3 structures, high bias voltage does not offer any particular advantages for O_2 detection.

Fig. 10 shows a temporal response of α-Ga_2O_3/$\varepsilon(\kappa)$-Ga_2O_3 structures to a 10% O_2 pulse at 180 °C and 5 V bias. It can be seen that the response signal is delayed and smeared out in time. It is worth noting that the delayed response is caused both by intrinsic and external factors such as the finite rate of O_2 concentration change in the analyte gas. According to our estimates it takes about one minute to establish a stationary value of O_2 concentration in the test chamber. The response time is likely to improve at higher bias voltages and higher operating temperatures, although further research is needed to verify this assumption.

D. Gas sensing mechanism

The following mechanisms can be proposed to explain the sensitivity of α-Ga_2O_3/$\varepsilon(\kappa)$-Ga_2O_3 structures to O_2.

First, O_2 molecules can change the height of the potential barrier at the Pt/Ga_2O_3 interface. In our previous work [13] we employed this mechanism to explain the H_2 sensitivity of the α-Ga_2O_3/$\varepsilon(\kappa)$-Ga_2O_3 structures. It was assumed that H_2 molecules catalytically dissociate into H atoms which then diffuse to the metal semiconductor interface. This process is very fast and efficient due to high solubility and diffusivity of hydrogen in Pt. The diffusion coefficient of H in Pt is 1.49×10^{-4} $cm^2 \times s^{-1}$ at room temperature and sharply increases with increasing temperature [22]. According to our estimates, H atoms can reach the metal/semiconductor interface in a time of about 10^{-6} s. The opposite picture is observed in the case of O_2. Indeed, O_2 molecules can adsorb and catalytically dissociate into atoms on Pt electrodes at temperatures above 175 °C. However, the diffusion coefficient of O in Pt is in the order of 10^{-17}-10^{-19} $cm^2 \times s^{-1}$ at 180 °C [23-25]. This means that it will take an extremely long time (10^8-10^{10} s) for the O atoms to diffuse through the Pt layer and reach the Pt/$\varepsilon(\kappa)$-Ga_2O_3 interface. Therefore, the reduction of the Schottky barrier height does not explain the sensitivity of samples to O_2.

The second possible mechanism involves interaction of O_2 molecules with oxygen vacancies V_O in the Ga_2O_3 layer. According to Fleischer and Meixner [26], V_O are frozen and cannot contribute to the gas sensitivity of β-Ga_2O_3 at temperatures below 600 °C. Due to the high diffusion barrier, the diffusion of V_O in β-Ga_2O_3 begins to appear at temperatures above 530 °C [27]. The behavior of V_O in α-Ga_2O_3 and $\varepsilon(\kappa)$-Ga_2O_3 is poorly studied, but it should not be very different from the properties of V_O in β-Ga_2O_3. Therefore, we assume that the diffusion of V_O in α-Ga_2O_3 and $\varepsilon(\kappa)$-Ga_2O_3 in the temperature range from 180 to 220 °C is highly unlikely. Thus, the mechanism of O_2 sensitivity due to V_O is unfeasible.

Finally, the electrical conductance of α-Ga_2O_3/$\varepsilon(\kappa)$-Ga_2O_3 structures can be modulated by chemisorption of O_2 molecules on the surface. According to SEM and XRD analysis, the $\varepsilon(\kappa)$-Ga_2O_3 phase has a pronounced grain structure. Potential barriers are formed between the grain boundaries due to the presence of surface states (SS). Holes in Ga_2O_3 exhibit very poor mobility, therefore bending of energy bands at the $\varepsilon(\kappa)$-Ga_2O_3 grain boundaries is caused by surface states with captured electrons. Energy band diagrams for an interface between two neighboring $\varepsilon(\kappa)$-Ga_2O_3 grains in equilibrium and at applied bias are shown in Fig. 11 a-b.

The voltage drop $\Delta U'$ per each grain in the one-dimensional case is given by the following equation [28]:

$$\Delta U' = \Delta U + J\rho_g(\gamma - 2W_d), \tag{2}$$

where ΔU is the voltage drop at the grain boundary; J is the current density; ρ_g is the specific volume resistance; γ is the length of one grain; W_d is the width of the SCR. The second term in the right part of expression (2) denotes the voltage drop on the grain bulk outside the SCR. In most of the cases the second term can be ignored because the resistance of the grain boundaries is much higher than the resistance of the material outside the SCR. In this case the structure can be regarded as a chain of resistances connected in series. Assuming that the grains are of the same size and the voltage drop is the same for all grains, the voltage drop across the entire film is give as:

$$U = \sum\nolimits_m \Delta U, \tag{3}$$

where $m = y/\gamma$ is the number of grains along the current path; y is the length of the film.

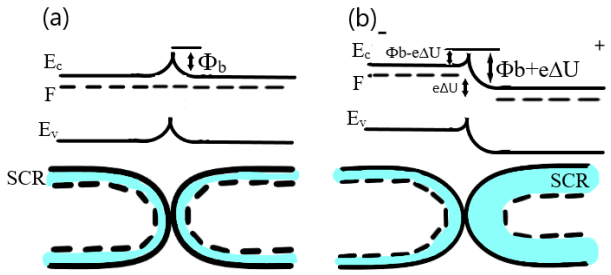

Fig. 11. Energy band diagrams for an interface of two neighboring $\varepsilon(\kappa)$-Ga_2O_3 grains in the equilibrium state (a) and at applied bias (b).

TABLE II
DEPENDENCE OF m ON TEMPERATURE

T, °C	*m*
180	0.150±0.003
200	0.089±0.003
220	0.160±0.006

In this case the current is given by the following expression [28]:

$$I = A * T^2 exp(-e\Phi_b/(kT))[eU/(kT)], \quad (4)$$

where $A*$ is the Richardson constant; Φ_b is the barrier height at the $\varepsilon(\kappa)$-Ga_2O_3 grain boundaries; k is the Boltzmann constant. According to the equation (4), the current is a linear function of the voltage. The experimentally observed nonlinear I–V dependence of the type $ln(I) \propto (U)^{0.25}$ which reflects the contribution of the reverse-biased Schottky barrier [18].

The differential resistance of the structure in a dry N_2 atmosphere R_{N2} can be obtained from equation (4) in the following form:

$$R_N = [dI/dU]^{-1} = [k/(A * \times T \times e)] \times exp[e\Phi_{bN2}/(kT)], \quad (5)$$

where Φ_{bN2} is the height of the barrier at the grain boundaries of $\varepsilon(\kappa)$-Ga_2O_3 in a dry N_2 atmosphere. With increasing C_{O2} in the chamber, the differential resistance of the structure α-Ga_2O_3/$\varepsilon(\kappa)$-Ga_2O_3 increases by the value $\Delta R = R_{O2} - R_{N2}$, where R_{O2} is the resistance of the sample at exposure of O_2. Based on this equality, we obtain the formula for ΔR:

$$\Delta R = R_{N2} \times [exp(e\Delta V_{O2}/(kT) - 1], \quad (6)$$

where $e\Delta V_{O2} = \Phi_{bO2} - \Phi_{bN2}$ is the change in the height of the barrier at the grain boundaries of $\varepsilon(\kappa)$-Ga_2O_3 at exposure of O_2; Φ_{bO2} is the height of the barrier at the grain boundaries of $\varepsilon(\kappa)$-Ga_2O_3 at exposure of O_2.

The dependence of $e\Delta V_{O2}$ on C_{O2} (Fig. 12) was calculated by using the expression (6). This dependence is approximated fairly accurately by a function of the form: $e\Delta V_{O2} \sim C_{O2}^m$, where m is a temperature-dependent exponent (Table II).

Thus, the O_2 sensitivity of α-Ga_2O_3/$\varepsilon(\kappa)$-Ga_2O_3 structures can be attributed to the variation of the energy barrier height at the grain boundaries of $\varepsilon(\kappa)$-Ga_2O_3 during dissociative chemisorption of O_2 molecules. The chemisorbed oxygen ions act as acceptor-like surface states. These states can easily

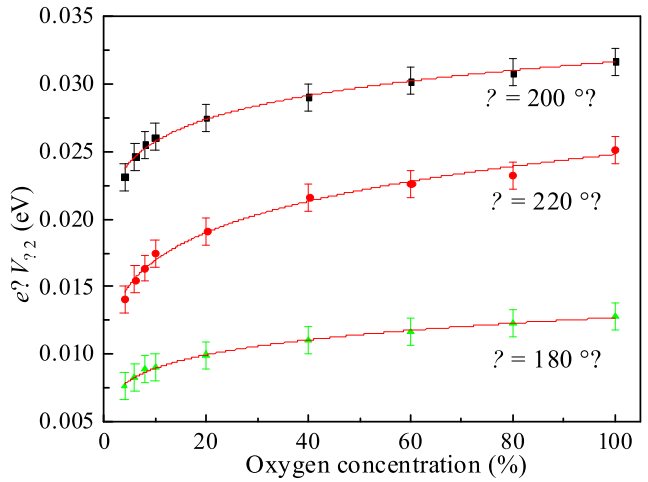

Fig. 12. Dependence of $e_1 V_{O2}$ on O_2 concentration at different temperatures.

capture electrons resulting in the increase of the energy barrier height between the grain boundaries and decrease of the current through the structure.

It is worth mentioning that the gas sensing model described above does not account for real microstructure of the specimens which were composed of columnar α-Ga_2O_3 domains surrounded by an $\varepsilon(\kappa)$-Ga_2O_3 matrix. Instead it was assumed that the films were single-phase and had a uniformly distributed grain structure. This assumption is perfectly valid because the current is transferred mainly through the $\varepsilon(\kappa)$-Ga_2O_3 phase. Indeed, Pt contact pads are in electrical contact with both α-Ga_2O_3 and $\varepsilon(\kappa)$-Ga_2O_3 phases. However, the α-Ga_2O_3 phase does not contribute much to the electrical conductivity of the film because it has a wider bandgap and forms isolated domains. The current flows along the path of least resistance, i.e. through the $\varepsilon(\kappa)$-Ga_2O_3. From this point of view, the use of PSS substrates and the presence of both α-Ga_2O_3 and $\varepsilon(\kappa)$-Ga_2O_3 polymorphs do not seem to be the determining factors for the presence of oxygen sensing properties. On the other hand, the growth on PSS was essential to produce $\varepsilon(\kappa)$-Ga_2O_3 layers [29]. The growth on planar sapphire substrates resulted in pure α-Ga_2O_3 phase which is insensitive to O_2. It is noteworthy that MSM structures based on pure $\varepsilon(\kappa)$-Ga_2O_3 films without α-Ga_2O_3 domains demonstrate sensitivity to gases at substantially higher temperatures (T >350 °C). It is not clear at the moment whether the gas sensitivity of α-Ga_2O_3/$\varepsilon(\kappa)$-Ga_2O_3 structures at low temperatures is related to the presence of α-Ga_2O_3 domains or is caused by some other factors.

According to the proposed sensing mechanism and experimental results, I_{N2} and I_{O2} increase with applied bias. The observed weak tendency to decrease the response with a rise of U from 7.5 to 100 V and to increase at U >100 V (Fig. 9) can be explained by the competition between contributions of SCR of grains to which a positive potential is applied (type 1) and SCR of grains to which a negative potential is applied (type 2). On the surface of type 1 grains, it is difficult for O_2 to capture electrons from the conduction band of the semiconductor. At U > 100 V, the width of the SCR of type

TABLE III
CHARACTERISTICS OF METAL OXIDE OXYGEN SENSORS

Material	Synthesis technique	Operating temperature range, °C	Dynamic range of concentration, %	Ref.
α-Ga_2O_3/ε(κ)-Ga_2O_3 on PSS	HVPE	180 - 220	2 - 100	This work
β-Ga_2O_3 thin film	Magnetron sputtering	900 - 1000	1 - 100	[7,10,31-34]
β-Ga_2O_3:Cr_2O_3 thin film	Magnetron sputtering	500 - 700	9 - 100	[11]
β-Ga_2O_3:SiO_x thin film	Magnetron sputtering	300 - 700	9 - 100	[35]
β-Ga_2O_3	Czochralski	700 - 1000	1 - 100	[36]
β-Ga_2O_3:M thin film, M = Ce; Sb; W, Zn	Sol–gel	420 - 520	0.01 - 1	[37]
β-Ga_2O_3 nanowires	Chemical thermal evaporation	200 - 500	0.5 - 5	[12]
$BaSnO_3$ thick film	Wet chem. synth.	700	1 - 20	[38]
$LaFeO_3$ thick film	Sol–gel	300 - 450	2 - 100	[39]
TiO_2/Pd thin film	Sol–gel	240	1 - 20	[40]
TiO_2/Ag thin film	Spray-pyrolysis	25 - 500	0.01 – 0.1	[41]
β-Ga_2O_3:Ti thin film	Magnetron sputtering	700	8 – 40 Pa	[42]

2 grains is so low, that stimulates the chemisorption of O_2, and as a result the response increases slightly.

Further research is needed to determine the role of the donor dopant concentration on the gas sensitivity of α-Ga_2O_3/$\varepsilon(\kappa)$-Ga_2O_3 structures. Kozhushner *et al.* [30] suggested that there is an optimum value of the electron concentration in n-type semiconductors which provides the highest sensitivity to gases. The electron concentration that is too low reduces the probability of surface states formation upon chemisorption of O_2 and other gases. When the electron concentration is too high, chemisorption of gases does not produce a significant change of the film resistance. On the other hand, highly doped Ga_2O_3 structures can exhibit gas sensitivity due to other mechanisms. For example, Pt-contacted α-Ga_2O_3/$\varepsilon(\kappa)$-Ga_2O_3 structures with a high donor concentration ($N_d \approx 4 \times 10^{18}$ cm^{-3}) showed strong response to H_2 due to modulation of the Schottky barrier height at the Pt/$\varepsilon(\kappa)$-Ga_2O_3 interface [13].

The α-Ga_2O_3/$\varepsilon(\kappa)$-Ga_2O_3 structures with moderate doping level (N_d =1.5-2.1 $\times 10^{17}$ cm^{-3}) studied in this work also showed high sensitivity to a relatively low concentration (0.745 %) of H_2 and CO in the operating temperature range of 180-220 °C and practically did not respond to NO_2 and CH_4 under the same experimental conditions. Compared to gas sensors based on β-Ga_2O_3 and other metal oxide semiconductors (Table III), α-Ga_2O_3/$\varepsilon(\kappa)$-Ga_2O_3 structures have significantly lower operating temperatures and wider dynamic range. However, α-Ga_2O_3/$\varepsilon(\kappa)$-Ga_2O_3 structures exhibited low and slow response.

IV. CONCLUSION

The electrical conductivity and gas sensing properties of α-Ga_2O_3/$\varepsilon(\kappa)$-Ga_2O_3 structures grown on patterned sapphire substrates by HVPE have been studied in the range of O_2 concentrations from 2 to 100 % and temperatures from 25 to 220 °C. O_2 exposure led to a reversible decrease in the current through α-Ga_2O_3/$\varepsilon(\kappa)$-Ga_2O_3 structures. It was shown that the sensitivity of structures to O_2 depended on the doping level. A significant increase of O_2 sensitivity in the temperature range from 180 to 220 °C and applied bias voltage below 7.5 V was observed when the concentration of Sn donors was decreased from $\sim 4 \times 10^{18}$ cm^{-3} to $\sim 1.5 \times 10^{17}$ cm^{-3}. The *I–V* characteristics of α-Ga_2O_3/$\varepsilon(\kappa)$-Ga_2O_3 MSM structures can be described by the theory of thermionic emission assuming that the diode approximation applies and the resistance of the semiconductor layer exceeds the resistance of the space charge regions at the metal/semiconductor interface. The gas sensing mechanism involves the chemisorption of O_2 molecules on the surface of $\varepsilon(\kappa)$-Ga_2O_3. As a result, the energy barrier at the grain boundaries of $\varepsilon(\kappa)$-Ga_2O_3 increases leading to a decrease in the current. The studied structures showed high sensitivity to relatively low concentrations (0.745 %) of H_2 and CO in the operating temperature range of 180-220 °C and exhibited practically no response to NO_2 and CH_4. The main advantage of O_2 sensors based on $\varepsilon(\kappa)$-Ga_2O_3 is sensitivity at relatively low temperatures in a wide dynamic range of O_2 concentrations.

REFERENCES

[1] X.-H. Kong, X.-F. Wang, and Q.-G. Liu, "Research on oxygen sensor for metallurgical process," *J. Iron Steel Res. Int.*, vol. 8, no. 1, pp. 60–62, Jan. 2001.

[2] U. Lampe, M. Fleischer, and H. Meixner, "Lambda measurement with Ga_2O_3," *Sens. Actuators B, Chem.*, vol. 17, no. 3, pp. 187–196, Feb. 1994, doi: 10.1016/0925-4005(93)00880-8.

[3] J. Fraden, *Handbook of Modern Sensors: Physics, Designs, and Applications*, 3rd ed. New York, NY, USA: Springer, 2004.

[4] A. Afzal, "β-Ga_2O_3 nanowires and thin films for metal oxide semiconductor gas sensors: Sensing mechanisms and performance enhancement strategies," *J. Mater.*, vol. 5, no. 4, pp. 542–557, Dec. 2019, doi: 10.1016/j.jmat.2019.08.003.

[5] M. Bartic, M. Ogita, M. Isai, C.-L. Baban, and H. Suzuki, "Oxygen sensing properties at high temperatures of β-Ga_2O_3 thin films deposited by the chemical solution deposition method," *J. Appl. Phys.*, vol. 102, no. 2, Jul. 2007, Art. no. 023709, doi: 10.1063/1.2756085.

[6] M. Bartic, Y. Toyoda, C.-I. Baban, and M. Ogita, "Oxygen sensitivity in gallium oxide thin films and single crystals at high temperatures," *Jpn. J. Appl. Phys.*, vol. 45, no. 6A, pp. 5186–5188, Jun. 2006, doi: 10.1143/JJAP.45.5186.

[7] C. Baban, Y. Toyoda, and M. Ogita, "Oxygen sensing at high temperatures using Ga_2O_3 films," *Thin Solid Films*, vol. 484, nos. 1–2, pp. 369–373, Jul. 2005, doi: 10.1016/j.tsf.2005.03.001.

[8] Y. Xu, X. Zhou, and O. T. Sorensen, "Oxygen sensors based on semiconducting metal oxides: An overview," *Sens. Actuators B, Chem.*, vol. 65, nos. 1–3, pp. 2–4, Jun. 2000, doi: 10.1016/S0925.4005(99)004219.

[9] R. Ramamoorthy, P. K. Dutta, and S. A. Akbar, "Oxygen sensors: Materials, methods, designs and applications," *J. Mater. Sci.*, vol. 38, pp. 4271–4282, Nov. 2003, doi: 10.1023/A:1026370729205.

[10] L.-T. Ju and S.-L. Ju, "Deposition of Ga_2O_3 thin film for high-temperature oxygen sensing applications," *J. Ovonic Res.*, vol. 8, no. 3, pp. 73–79, May/Jun. 2012.
[11] A. V. Almaev, E. V. Chernikov, N. A. Davletkildeev, and D. V. Sokolov, "Oxygen sensors based on gallium oxide thin films with addition of chromium," *Superlattices Microstructures*, vol. 139, Mar. 2020, Art. no. 106392, doi: 10.1016/j.spmi.2020.106392.
[12] Z. Liu, T. Yamazaki, Y. Shen, T. Kikuta, N. Nakatani, and Y. Li, "O_2 and CO sensing of Ga_2O_3 multiple nanowire gas sensors," *Sens. Actuators B, Chem.*, vol. 129, no. 2, pp. 666–670, Feb. 2008, doi: 10.1016/j.snb.2007.09.055.
[13] A. V. Almaev *et al.*, "Hydrogen influence on electrical properties of Pt-contacted α-Ga_2O_3/ϵ-Ga_2O_3 structures grown on patterned sapphire substrates," *J. Phys. D, Appl. Phys.*, vol. 53, no. 41, Jul. 2020, Art. no. 414004, doi: 10.1088/1361-6463/ab9c69.
[14] S. Shapenkov *et al.*, "Halide vapor phase epitaxy α- and ϵ-Ga_2O_3 epitaxial films grown on patterned sapphire substrates," *Phys. Status Solidi*, vol. 217, no. 14, Jul. 2020, Art. no. 1900892, doi: 10.1002/pssa.201900892.
[15] E. Ahmadi and Y. Oshima, "Materials issues and devices of α- and β-Ga_2O_3," *J. Appl. Phys.*, vol. 126, no. 16, Oct. 2019, Art. no. 160901, doi: 10.1063/1.5123213.
[16] Y. Qin *et al.*, "High-performance metal-organic chemical vapor deposition grown β-Ga_2O_3 solar-blind photodetector with asymmetric schottky electrodes," *IEEE Electron Device Lett.*, vol. 40, no. 9, pp. 1475–1478, Sep. 2019, doi: 10.1109/LED.2019.2932382.
[17] A. G. Milnes and D. L. Feucht, *Heterojunctions and Metal-Semiconductor Junctions*. New York, NY, USA: Academic, 1972.
[18] H. Elhadidy, J. Sikula, and J. Franc, "Symmetrical current–voltage characteristic of a metal–semiconductor–metal structure of Schottky contacts and parameter retrieval of a CdTe structure," *Semicond. Sci. Technol.*, vol. 27, no. 1, Dec. 2011, Art. no. 015006, doi: 10.1088/0268-1242/27/1/015006.
[19] A. Y. Polyakov *et al.*, "Editors' choice—Electrical properties and deep traps in β-Ga_2O_3:Sn films grown on sapphire by halide vapor phase epitaxy," *ECS J. Solid State Sci. Technol.*, vol. 9, no. 4, Apr. 2020, Art. no. 045003, doi: 10.1149/2162-8777/ab89bb.
[20] V. I. Nikolaev *et al.*, "Thick epitaxial α-Ga_2O_3:Sn layers on a patterned sapphire substrate," *Tech. Phys. Lett.*, vol. 46, no. 3, pp. 228–230, Mar. 2020, doi: 10.1134/S106378502003013X.
[21] A. V. Almaev *et al.*, "Effect of ambient humidity on the electrical conductivity of polymorphic Ga_2O_3 structures," *Semiconductors*, vol. 55, no. 3, pp. 346–353, Mar. 2021, doi: 10.1134/S1063782621030027.
[22] W.-J. Liu, B.-L. Wu, and C.-S. Cha, "Determination of surface diffusion coefficients of the hydrogen adatom and surface oh radical on platinum electrode," *Russian J. Electrochem.*, vol. 36, no. 8, pp. 846–851, Aug. 2000, doi: 10.1007/BF02757057.
[23] J. V. Barth, "Transport of adsorbates at metal surfaces: From thermal migration to hot precursors," *Surf. Sci. Rep.*, vol. 40, nos. 3–5, pp. 75–149, Oct. 2000, doi: 10.1016/S0167-5729(00)00002-9.
[24] R. Schmiedl *et al.*, "Oxygen diffusion through thin Pt films on Si(100)," *Appl. Phys. A, Solids Surf.*, vol. 62, no. 3, pp. 223–230, Mar. 1996, doi: 10.1007/BF01575085.
[25] L. R. Velho and R. W. Bartlett, "Diffusivity and solubility of oxygen in platinum and Pt-Ni alloys," *Metall. Mater. Trans. B*, vol. 3, no. 1, pp. 65–72, Jan. 1972, doi: 10.1007/BF02680586.
[26] M. Fleischer and H. Meixner, "Characterization and crystallite growth of semiconducting high-temperature-stable Ga_2O_3 thin films," *J. Mater. Sci. Lett.*, vol. 11, no. 24, pp. 1728–1731, 1992, doi: 10.1007/BF00736223.
[27] A. Kyrtsos, M. Matsubara, and E. Bellotti, "Migration mechanisms and diffusion barriers of vacancies in Ga_2O_3," *Phys. Rev. B, Condens. Matter*, vol. 95, no. 24, Jun. 2017, Art. no. 245202, doi: 10.1103/PhysRevB.95.245202.
[28] A. Fahrenbruch and R. Bube, *Fundamentals of Solar Cells: Photovoltaic Solar Energy Conversion*. New York, NY, USA: Elsevier, 1983.
[29] V. I. Nikolaev *et al.*, "HVPE growth and characterization of ϵ-Ga_2O_3 films on various substrates," *ECS J. Solid State Sci. Technol.*, vol. 9, no. 4, May 2020, Art. no. 045014, doi: 10.1149/2162-8777/ab8b4c.
[30] M. A. Kozhushner, V. L. Bodneva, and L. I. Trakhtenberg, "Sensor effect theory for the detection of reducing gases," *Russian J. Phys. Chem. A*, vol. 86, no. 8, pp. 1281–1287, Jun. 2012, doi: 10.1134/S0036024412080055.
[31] M. Fleischer, W. Hanrieder, and H. Meixner, "Stability of semiconducting gallium oxide thin films," *Thin Solid Films*, vol. 190, no. 1, pp. 93–102, Sep. 1990, doi: 10.1016/0040-6090(90)90132-W.
[32] M. Ogita, K. Higo, Y. Nakanishi, and Y. Hatanaka, "Ga_2O_3 thin films for oxygen sensors at high temperature," *Appl. Surf. Sci.*, vols. 175–176, pp. 721–725, May 2001, doi: 10.1016/S0169-4332(01)00080-0.
[33] M. Ogita, N. Saika, Y. Nakanishi, and Y. Hatanaka, "Ga_2O_3 thin films for high-temperature gas sensors," *Appl. Surf. Sci.*, vol. 142, pp. 188–191, Apr. 1999, doi: 10.1016/S0169-4332(98)00714-4.
[34] C.-I. Baban, Y. Toyoda, and M. Ogita, "High temperature oxygen sensor using a Pt-Ga_2O_3-Pt sandwich structure," *Jap. J. Appl. Phys.*, vol. 43, no. 10, pp. 7213–7216, Oct. 2004, doi: 10.1143/JJAP.43.7213.
[35] A. V. Almaev, E. V. Chernikov, B. O. Kushnarev, N. N. Yakovlev, P. M. Korusenko, and S. N. Nesov, "Oxygen sensors based on thin films of gallium oxide modified with silicon," *Proceedings*, vol. 42, no. 1, p. 4, Nov. 2019, doi: 10.3390/ecsa-6-06549.
[36] M. Bartic, "Mechanism of oxygen sensing on β-Ga_2O_3 single-crystal sensors for high temperatures," *Phys. Status Solidi A*, vol. 213, no. 2, p. 457–462, 2016, doi: 10.1002/pssa.201532599.
[37] Y. Li *et al.*, "Investigation of the oxygen gas sensing performance of Ga_2O_3 thin films with different dopants," *Sens. Actuators B, Chem.*, vol. 93, no. 1-3, pp. 431–434, Aug. 2003, doi: 10.1016/S0925-4005(03)00171-0.
[38] J. Cerdà *et al.*, "Perovskite-type $BaSnO_3$ powders for high temperature gas sensor applications," *Sens. Actuators B, Chem.*, vol. 84, no. 1, pp. 21–25, Apr. 2002, doi: 10.1016/S0925-4005(02)00005-9.
[39] I. Jaouali *et al.*, "$LaFeO_3$ ceramics as selective oxygen sensors at mild temperature," *Ceram. Int.*, vol. 44, no. 4, pp. 4183–4189, Mar. 2018, doi: 10.1016/j.ceramint.2017.11.221.
[40] H. Wang, L. Chen, J. Wang, Q. Sun, and Y. Zhao, "A micro oxygen sensor based on a nano sol-gel TiO_2 thin film," *Sensors*, vol. 14, no. 9, pp. 16423–16433, Sep. 2014, doi: 10.3390/s140916423.
[41] L. Castañeda, A. López-Suárez, and A. Tiburcio-Silver, "Influence of colloidal silver nanoparticles on the novel flower-like titanium dioxide oxygen sensor performances," *J. Nanosci. Nanotechnol.*, vol. 10, no. 2, pp. 1343–1348, Feb. 2010, doi: 10.1166/jnn.2010.1839.
[42] S. Manandhar, A. K. Battu, A. Devaraj, V. Shutthanandan, S. Thevuthasan, and C. V. Ramana, "Rapid response high temperature oxygen sensor based on titanium doped gallium oxide," *Sci. Rep.*, vol. 10, no. 1, Jan. 2020, Art. no. 178, doi: 10.1038/s41598-019-54136-8.

Nikita N. Yakovlev is currently pursuing the master's degree with Tomsk State University. His current research interests focus on devices-based on the various polymorphs of gallium oxide.

Vladimir I. Nikolaev received the M.S. degree in physics of metals from Peter the Great St. Petersburg Polytechnic University, Russia, in 1981, and the Ph.D. degree in solid state physics from the Ioffe Institute, St. Petersburg, Russia, in 1989. From 1993 to 1996, he worked as a Researcher with Cree EED. From 2009 to 2013, he was the Head of the Research and Development Department, Optogan LLC. From 2013 to 2019, he was an Assistant Professor with ITMO University. He is currently the Head of the Physics of Shaped Crystals Laboratory, Ioffe Institute. He is also the Founder and CEO of Perfect Crystals LLC, a research spin-off company aimed at the development of wide bandgap semiconductors. He has published more than 300 scientific articles in peer-reviewed international journals and conferences, and has six granted patents. He is the author of several chapters in books on electronics and smart materials. He was awarded the Prize of the Physical Society of the Ioffe Institute for the discovery of the electro-plastic effect in ferroelectric crystals, in 1990. He is in the Editorial Board of the *Technical Physics* journal.

Sergey I. Stepanov received the M.S. degree in optoelectronics from Saint Petersburg Electrotechnical University, Russia, in 1996, and the Ph.D. degree in physics from the University of Bath, U.K., in 2003. He has held various research positions at Cree EED, Bath University, IQE, and ITMO University. He is currently a Research Scientist with the Ioffe Institute. He has authored several chapters in scientific books and numerous research articles in refereed journals. His research interests include physics of semiconductor devices, wide bandgap semiconductors, crystal growth, and epitaxy.

Aleksei V. Almaev received the Ph.D. degree in physical and mathematical sciences, in 2018. He is currently the Head of the Laboratory of Advanced Materials for Gas and Chemical Sensors, Research and Development Center for Advanced Technologies in Microelectronics, Tomsk State University. His research interests include research of gallium oxide and related devices.

Aleksei I. Pechnikov received the M.S. degree in electric engineering from Saint Petersburg Electrotechnical University "LETI," Russia. He started his career in the field of semiconductor technology in 1999. Since 1999, he held various positions at Technologies and Devices International, Inc., USA, Nitronix, USA, and Optogan, Russia. He currently works with Perfect Crystals LLC and the Ioffe Institute, St. Petersburg, Russia. He has a vast experience in GaN and Ga2O3 epitaxial growth by HVPE and MOCVD techniques. He has published over 40 research articles.

Evgeny V. Chernikov is currently the Leading Process Engineer with the Laboratory of Advanced Materials for Gas and Chemical Sensors, Research and Development Center for Advanced Technologies in Microelectronics, National Research Tomsk State University. His research interests are focused on the technology of metal oxide thin films and research of their surface properties and characteristics.

Bogdan O. Kushnarev is currently pursuing the master's degree with the Department of Semiconductor Electronics, Tomsk State University. His current research interests focus on gas sensing devices-based on gallium and chromium oxides.